energy&fuels

Article

Cite This: *Energy Fuels* 2018, 32, 10100−10105

pubs.acs.org/EF

Flame Inhibition Chemistry: Rate Coefficients of the Reactions of HBr with CH_3 and OH Radicals at High Temperatures Determined by Quasiclassical Trajectory Calculations

Szabolcs Góger,[†,‡] Péter Szabó,[§] Gábor Czakó,[∥] and György Lendvay*[,†,‡]

[†]Department of General and Inorganic Chemistry, University of Pannonia, Egyetem utca 10, Veszprém H-8200, Hungary

[‡]Institute of Materials and Environmental Chemistry, Research Centre for Natural Sciences, Hungarian Academy of Sciences, Magyar tudósok körútja 2, Budapest H-1117, Hungary

[§]Applied Physics, Division of Materials Science, Department of Engineering Science and Mathematics, Luleå University of Technology, 97187 Luleå, Sweden

[∥]Department of Physical Chemistry and Materials Science, Institute of Chemistry, University of Szeged, Rerrich Béla tér 1, Szeged H-6720, Hungary

ABSTRACT: Reactions of HBr with radicals are involved in atmospheric chemistry and in the mechanism of operation of bromine-containing flame retardants. The rate coefficients for two such reactions, HBr + OH and HBr + CH_3, are available from earlier experiments at near or below room temperature, relevant for atmospheric chemistry, and in this domain, the activation energy for both has been found to be negative. However, no experimental data are available at combustion temperatures. In this work, to provide reliable data needed for modeling the action of brominated flame suppressants, we used the quasiclassical trajectory (QCT) method in combination with high-level *ab initio* potential energy surfaces to evaluate the rate coefficients of the two title reactions at combustion temperatures. The QCT calculations have been validated by reproducing the experimental rate coefficients at room temperature. At temperatures between 600 and 3200 K, the QCT rate coefficients display positive activation energies. We recommend the following extended Arrhenius expressions to describe the temperature dependence of the thermal rate coefficients: $k_6 = (9.86 \pm 2.38) \times 10^{-16} T^{(1.23\pm0.03)} \exp[(5.93 \pm 0.33)\ \text{kJ mol}^{-1}/RT]\ \text{cm}^3\ \text{molecule}^{-1}\ \text{s}^{-1}$ for the HBr + OH → H_2O + Br reaction, and $k_{-2} = (4.06 \pm 2.72) \times 10^{-18} T^{(1.83\pm0.08)} \exp[(7.53 \pm 0.18)\ \text{kJ mol}^{-1}/RT]\ \text{cm}^3\ \text{molecule}^{-1}\ \text{s}^{-1}$ for the HBr + CH_3 → CH_4 + Br reaction. The latter is in very good agreement with the formula proposed by Burgess et al. [Burgess, D. R., Jr.; Babushok, V. I.; Linteris, G. T.; Manion, J. A. A Chemical Kinetic Mechanism for 2-Bromo-3,3,3-trifluoropropene (2-BTP) Flame Inhibition. *Int. J. Chem. Kinet.* **2015**, *47*, 533−619, DOI: 10.1002/kin.20923]. The conventional transition state theory has been tested against the rate data obtained by the QCT method and was found to overestimate not only the rate coefficients but also the activation energies.

INTRODUCTION

Significant effort in combustion chemistry is devoted to understanding the mode of action of flame retardants and other fire suppressants. Flame retardation can be achieved by physical means (especially cooling), but the disruption of the chemistry of combustion is often more efficient and comes with less side effects. Some fire suppressants, for example, CO_2, simply prevent the contact of the flammable material with oxygen. More sophisticated are chemically active flame retardants that produce radicals that interfere with the chain reactions in which the combustible material is consumed and energy is released. This latter class is represented by the probably most widely known flame suppressants, compounds containing bromine atom(s). Hundreds of tonnes of brominated flame retardants are used every year in the polymer industry as additives.[1,2] In everyday life, halons, halogenated hydrocarbons, were extensively used as fire extinguishers until recently. Among them, Halon 1301, CF_3Br, is still the most efficient and fulfills numerous other requirements: it is easy to deploy, is not poisonous to humans, does not form aggressive byproducts when used, etc. However, unfortunately, CF_3Br is rather harmful when released to the atmosphere: it is among the most efficient ozone-depleting substances and has a large global warming potential. Because of these properties, CF_3Br and two other halons were in the second group of substances[3] banned under the Montreal Protocol as of 1994, so that halon production for firefighting purposes ceased by the year 2000. Substitutes for halons have actively been searched for more than 2 decades. However, in commercial and military aviation and some special industrial applications, there is still no appropriate replacement,[4−6] so that in these "essential use" areas, CF_3Br will not be phased out before about 2040. This means that the about 45 000 tonnes of Halon 1301, the balance left of the cumulative global production by 2010 (ca. 150 000 metric tonnes), will be in use until fully consumed. The most promising substitute, C_2F_5H, (HFC-125), has been banned by the Kigali Amendment to the Montreal Protocol.[7] The next most promising alternative, 2-bromo-3,3,3-trifluoropropene (2-

Special Issue: SMARTCATs COST Action

Received: March 23, 2018
Revised: May 5, 2018
Published: May 8, 2018

DOI: 10.1021/acs.energyfuels.8b00989
Energy Fuels 2018, 32, 10100−10105

BTP), similar to CF_3Br and the brominated flame retardants used in the polymer industry, also contains Br atoms. Because it seems that brominated fire suppressants will be around for decades, it is important to understand their mechanism of action, which has common features for all such compounds and lends them their exceptional efficiency. Deep insight into their flame chemistry can be expected to be of help in the continuing search for halon substitutes. Modeling plays an essential role in understanding the interference of combustion chemistry of fuels and brominated fire suppressants. The efforts thus far concentrated primarily on CF_3Br,[8−10] but the chemical mechanism, with appropriate extensions, can be applied to other bromine-containing compounds.

It has been established that the steps responsible for flame inhibition by brominated compounds are common, irrespective of the type of fuel, and that the active species are Br and HBr, which participate in the cycle:[11,12]

$$H + HBr \rightarrow H_2 + Br \quad (R1)$$

$$Br + CH_4 \rightarrow HBr + CH_3 \quad (R2)$$

$$Br + CH_2O \rightarrow HCO + HBr \quad (R3)$$

$$Br + HCO \rightarrow CO + HBr \quad (R4)$$

$$H + Br + M \rightarrow HBr + M \quad (R5)$$

$$OH + HBr \rightarrow Br + H_2O \quad (R6)$$

The net effect is conversion of two free H atoms into H_2, i.e., removal of the chain-carrying H atoms. This is the major factor responsible for the flame inhibition efficiency of brominated fire suppressants.

In a recent study, Burgess et al.[12] presented a detailed kinetic model of the flame inhibition chemistry of 2-BTP, $CF_3CBr{=}CH_2$. In the mechanism, two reactions of HBr with radicals ubiquitous in flames, namely, reaction R6 and the reverse of reaction R2

$$HBr + CH_3 \rightarrow Br + CH_4 \quad (R-2)$$

have also been included, with estimated rate coefficients. Both reactions are well-known in atmospheric chemistry, where they have an important role in the adverse effect of CF_3Br on the stratospheric ozone layer. Their rate coefficients were measured at low temperatures relevant in atmospheric chemistry and were found to decrease with an increasing temperature below about 300 K: k_6 in the 50−300 K range and k_{-2} in the 200−300 K range, with a reduced slope above 300 K. No direct experiments have been performed at flame temperatures. The extrapolation of the decreasing tendency of the below room temperature experimental rate coefficients to higher temperatures was used in earlier modeling of flame inhibition by brominated fire suppressants.[9−11] However, on the basis of experience with related reactions, one can expect that, at flame temperatures, the rate coefficient of neither of these reactions should decrease with increasing temperature. Burgess et al.[12] recently reviewed the scarce information on the high-temperature rate constants for reactions R6 and R−2 and intuitively proposed that both should have positive temperature dependence at flame temperatures. They gave estimated rate expressions for both

$$k_6^{est} = 2.05 \times 10^{11} T^{0.58\pm0.17} \exp[(1.4 \pm 0.1)\ \text{kJ mol}^{-1}/RT]\ \text{cm}^3\ \text{mol}^{-1}\ \text{s}^{-1} \quad (1)$$

and

$$k_{-2}^{est} = 2.10 \times 10^{7} T^{1.57} \exp[6.0\ \text{kJ mol}^{-1}/RT]\ \text{cm}^3\ \text{mol}^{-1}\ \text{s}^{-1} \quad (2)$$

The proposed change of direction of the temperature dependence of the rate coefficients is not unexpected and is supported by the nature of the potential energy surfaces (PES) of both reactions[13,14] (Figure 1).

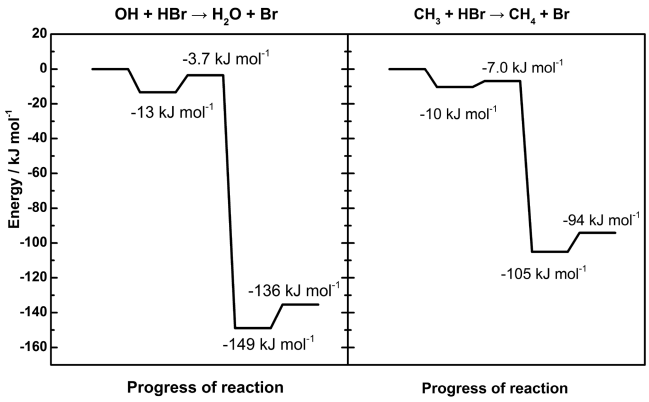

Figure 1. Potential energy profiles of reactions OH + HBr (reaction R6) and CH_3 + HBr (reaction R−2) (on the basis of refs 13 and 14, respectively), showing the common characteristics: a van der Waals well corresponding to a pre-reaction complex, a submerged barrier, and significant exothermicity.

The reactants in both of them have a propensity to form a van der Waals complex, which means that the potential energy decreases when either radical approaches a HBr molecule and there is a potential well corresponding to the complex. Quantum chemical calculations[13−15] support this assumption; moreover, they show that the top of the potential barrier separating the van der Waals complex of the reactants from the products (Br + H_2O for reaction R6 and Br + CH_4 for reaction R−2) is below the reactant level. The rate coefficient of this kind of reaction is known[16,17] to display a change of sign of the activation energy from negative at low temperatures to positive at high temperatures. Such a behavior has been observed for reaction R−2 by Chen et al.,[18] who used the Rice−Ramsperger−Kassel−Marcus (RRKM) variant of the transition state theory (TST), and Krasnoperov et al.,[19] who used the version of TST in which energy levels below the entrance level were not included in the number of states of the transition state. Note that both of these works involved only relatively low temperatures. The aim of the present work is to investigate the magnitude and temperature dependence of the rate coefficients of both reactions by performing precise reaction dynamical calculations using PES derived from high-level *ab initio* quantum chemical calculations. On the basis of the results, we propose extended Arrhenius expressions that can be used to assess or improve the estimates by Burgess et al., with the intent of helping to ensure the reliability of flame inhibition modeling.

METHODS

Quasiclassical Trajectory (QCT) Calculations. We have used two theoretical methods in this work: QCT calculations and TST. In QCT calculations,[20] we solve the classical equations of motion for each atom participating in the reaction. The forces are obtained as negative gradients of a potential energy function, which depends upon the coordinates of all atoms in the system and is generally referred to as

DOI: 10.1021/acs.energyfuels.8b00989
Energy Fuels 2018, 32, 10100−10105

potential energy (hyper)surface (PES). To simulate the quantized nature of the vibration and rotation of the reactant molecules, the internal motion of molecules is described by ensembles of classical states that correspond to preselected quantum mechanical states. The rate coefficient representing the average behavior of thermal ensembles was evaluated by Monte Carlo integration. Among the initial conditions of trajectories, those corresponding to the internal states of the reactant molecules were selected at random from the ensembles described above. The collision energy was taken by sampling the Maxwell−Boltzmann distribution corresponding to the given temperature. The impact parameter b was sampled with a weight proportional to b itself. With such settings, the calculation of the rate coefficient is reduced to counting the ratio of reactive events to that of all attempts. In this work, we have calculated 200 000 trajectories at each temperature. The integration time step was 0.1 and 0.07 fs in the calculations on reactions R6 and R−2, respectively, guaranteeing energy conservation better than 0.05 kJ mol^{-1}. The maximum impact parameter was set to 6 Å below 1500 K and to 4 Å at temperatures higher than 1500 K for both reactions, so that the reactive count was about 5−10%. The error bars of the QCT rate coefficients were calculated as follows: The 200 000 trajectories were run as 64 independent batches consisting of 3125 trajectories each; their results were treated as those of 64 separate "measurements" having normally distributed errors; and the standard deviation was calculated according to this setup. The other details of the QCT calculations are the same as described in our recent papers.[21−23]

TST. Because we have reliable rate coefficients from reaction dynamical calculations, we have the opportunity to test the performance of conventional TST. If, in agreement with the principles of the theory, one assumes that the reacting system is in equilibrium during the reaction, then the complex formation can be treated as preliminary equilibrium (the assumption that the complex is in equilibrium is the basis of all statistical theories, including the more sophisticated variational TST methods; however, it is probably not fulfilled for a van der Waals complex, which means that statistical theories remain an approximation for such reactions). With this assumption, the rate coefficient is the product of the equilibrium constant of complex formation (K_{cmplx}) and the rate coefficient of the reaction from the complex to products (k_{abs}). When one expresses the two factors via the partition function of the reactants, the complex and the transition state (which is placed on top of the potential barrier), the rate coefficient becomes

$$k_r = K_{cmplx}k_{abs} = \frac{Q_{cmplx}}{Q_{rea}}\exp\left(-\frac{V_{cmplx}-V_{rea}}{k_BT}\right)\kappa\frac{k_BT}{h}$$
$$\frac{Q_{TS}}{Q_{cmplx}}\exp\left(-\frac{V_{TS}-V_{cmplx}}{k_BT}\right) = \kappa\frac{k_BT}{h}\frac{Q_{TS}}{Q_{rea}}\exp\left(-\frac{V_{TS}-V_{rea}}{k_BT}\right) \quad (3)$$

where Q_i and V_i are the partition function and energy level of species i, with i = rea, cmplx, or TS for the reactants, their van der Waals complex, and the transition state, k_B and h are Boltzmann's and Planck's constants, T is the temperature, and κ stands for the transmission coefficient accounting for tunneling, calculated in this work with the simple Wigner formula.[24] The tunneling factor was found to be essentially unity at temperatures above 500 K. As a result of the assumption of preliminary equilibrium, the partition function of the complex and the energy level V_{cmplx} disappear in eq 3 and the rate coefficient is the same as if the complex was not there at all. This means that the rate is determined solely by the properties of the reactants and the submerged potential barrier. The partition functions are generally calculated using the rigid rotor−harmonic oscillator approximation. More sophisticated statistical rate theories are available, which provide more accurate rate coefficients than conventional TST, but extensive method testing is not the purpose of this work.

PES. For both reactions, we used analytical PES functions obtained by fitting to a large number of high-level *ab initio* energy points. Both functions were taken from the literature, and both are invariant to the permutation of like atoms. For the OH + HBr → H_2O + Br reaction, we used the PES fitted by de Oliveira-Filho et al.[13,15] The OH radical has four spin−orbit states, and with the appearance of the HBr molecule, an individual potential surface starts from each of them. According to the *ab initio* calculations, of the four surfaces, only one is reactive. This has been taken into account by dividing the rate coefficients calculated on the single reactive surface by a factor of 4.

The CH_3 + HBr trajectories were run on a slightly modified version of the full-dimensional spin−orbit ground-state PES developed by one of us.[14] The modification is based on new *ab initio* energies calculated at the same level of theory as used previously [a composite method including relativistic correction, yielding CCSDT(Q)/complete-basis-set quality energies, see ref 14] at 5000 additional geometries. The latter characterizes the entrance valley to the CH_3−HBr van der Waals well, where the original version was less accurate, because this region was not of interest in the previous study. In 2000 of these points, the C−H−Br triplet was arranged along a straight line. The geometries of CH_3 and HBr were selected using normal mode sampling (with the modification that instead of the phase of the oscillators, the normal mode displacement was sampled uniformly). The entire set of energies, including the original 21 574 points complemented by the 5000 energies calculated in this work, were fitted with the same method previously.[25]

To validate the QCT method−PES combinations, the rate coefficients have been calculated using the QCT method at 300 K, which is in the low-temperature region, where experimental data are available. The obtained rate coefficients were found to agree within experimental accuracy with the experimental values for both reactions and with that of de Oliveira-Filho et al.[13,15] for reaction R6. The production calculations were performed only above 600 K, because rate coefficients at lower temperatures can be found in the cited papers.[13,15]

RESULTS

The rate coefficients obtained with the TST and QCT methods between 600 and 3000 K are shown in Figures 2 and 3, together with the available experimental data for reaction R6[26] and reaction R−2,[27−34] respectively. The error bars on the QCT points represent ±1 standard deviation.

The results calculated at 300 K for validation are shown as points without error bars in Figures 2 and 3. They agree very well with the experimental data (note the linear ordinate scale

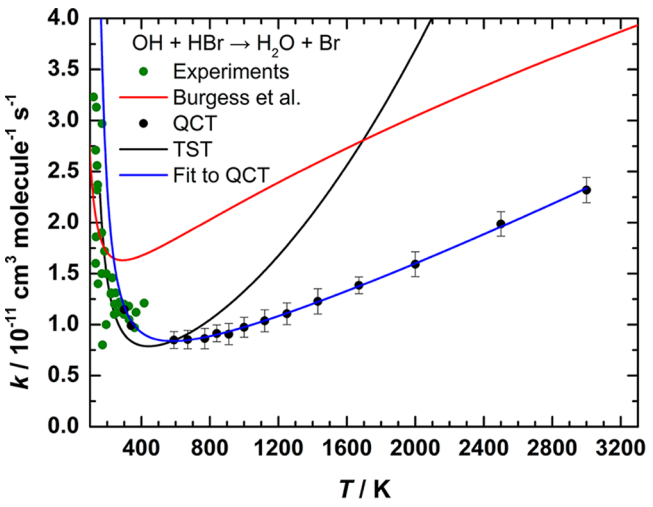

Figure 2. Temperature dependence of the calculated rate coefficients of reaction OH + HBr → H_2O + Br (reaction R6). The experimental data (green dots) are taken from the review of Mullen and Smith.[26] Black dots, QCT results; blue line, fit to QCT data according to eq 5; black line, TST results; and red line, rate coefficient estimated by Burgess et al.,[12] (eq 1).

DOI: 10.1021/acs.energyfuels.8b00989
Energy Fuels 2018, 32, 10100−10105

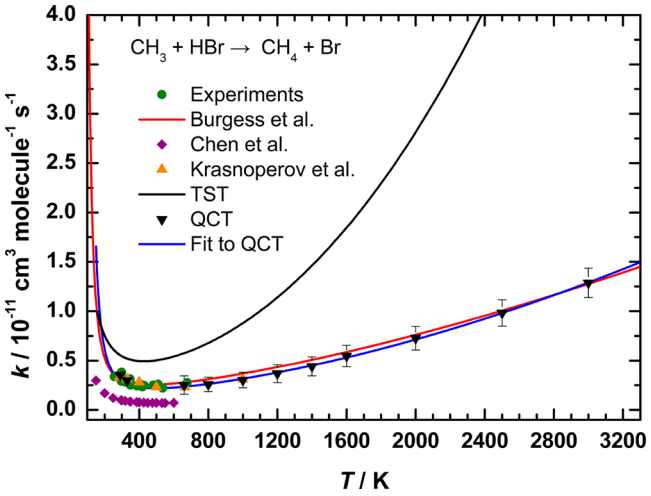

Figure 3. Temperature dependence of the calculated rate coefficients of reaction CH_3 + HBr → CH_4 + Br (reaction R−2). The experimental data are taken from refs 27−34. Black dots, QCT results; blue line, fit to QCT data according to eq 6; black line, TST results; red line, rate coefficient estimated by Burgess et al.,[12] (eq 2). The high-temperature end of the results of Krasnoperov et al.[19] and Chen et al.[18] are also shown.

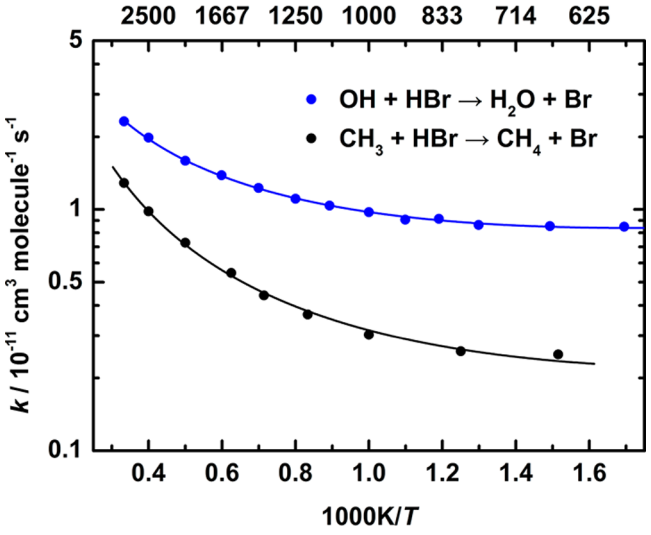

Figure 4. Rate coefficients of reactions R6 and R−2 in Arrhenius representation. The continuous lines correspond to the fits shown in eqs 5 and 6.

in the figures) and, in the case of CH_3 + HBr, with the theoretical results of Krasnoperov et al.[19] The QCT calculations justify the expectation that, in the high-temperature region, the rate coefficient has a positive temperature dependence, in contrast with the low-temperature behavior. The behavior of the rate coefficients obtained in the TST calculations is qualitatively the same. For reaction R6, the TST curve also matches the experiments at low temperatures (200−300 K) and the QCT rates at about 600 K, but above that, its slope is much larger than that of the QCT curve and the rate coefficient is overestimated by about a factor of 2 and 3 at 1500 and 2500 K, respectively. For reaction R−2, the TST rate coefficients overestimate the experimental and QCT results in the entire temperature range and are larger by a factor of 2, 3, and 4.5 at 600, 1500, and 2500 K, respectively.

In the Arrhenius representation shown in Figure 4, one can see that neither of the two reactions obeys a single linear Arrhenius law, even in the limited range where the rate coefficient increases monotonously. We have therefore used the extended Arrhenius (also called Kooij) equation

$$k = A_x T^n \exp\left(-\frac{B}{RT}\right) \tag{4}$$

to fit our data points (Figures 2−4). In eq 4 R is the gas constant, T is the absolute temperature, and A_x, n, and B are fitting parameters. Note that the two lowest temperature QCT points have not been included in the high-temperature fits, because they are in the negative activation energy part of the temperature regime, which is out of scope of the present study. On the basis of our calculations, the suggested rate coefficients in the 500−3200 K range for reactions R−2 and R6 are the following (the uncertainties given correspond to one standard deviation):

$$k_6 = (9.86 \pm 2.38) \times 10^{-16} T^{(1.23\pm0.03)} \exp[(714 \pm 40)/T] \text{ cm}^3 \text{ molecule}^{-1} \text{ s}^{-1} \tag{5}$$

and

$$k_{-2} = (4.06 \pm 2.72) \times 10^{-18} T^{(1.83\pm0.08)} \exp[(906 \pm 22)/T] \text{ cm}^3 \text{ molecule}^{-1} \text{ s}^{-1} \tag{6}$$

The exponential parameter $B = E_x/R$ corresponds to $E_{x,-2}$ = −5.9 ± 0.3 kJ mol^{-1} and $E_{x,6}$ = −7.3 ± 0.18 kJ mol^{-1}, respectively. The large deviation of parameter n from 0 corresponds to the large curvature of the Arrhenius plot (Figure 4), i.e., to significant temperature dependence of the experimental activation energy. Application of the quantitative definition of the latter[35]

$$E_a = -R\frac{\partial \ln k}{\partial 1/T} \tag{7}$$

to the extended Arrhenius expression yields

$$E_a = (nT - B)R \tag{8}$$

i.e., the activation energy increases linearly with the temperature. The numerical values for 1000, 1500, and 2000 K are 16.1, 21.3, and 26.4 kJ mol^{-1} for OH + HBr → H_2O + Br and 22.7, 30.6, and 38.0 kJ mol^{-1} for CH_3 + HBr → CH_4 + Br, respectively. The remarkable change indicates that predominantly dynamical factors determine the temperature dependence of the reaction rate for both processes.

DISCUSSION

The rate coefficients obtained using the QCT method match the high-temperature end (around room temperature) of the experimental measurements and/or the earlier QCT calculations for both reactions. This indicates that the potential surfaces and the method used in the dynamical calculations are accurate enough to provide reliable data at high temperatures. We expect that tunneling, a quantum effect not captured by the QCT method, does not have a significant role in these reactions because, first, the potential barrier is low and wide and, second, we are interested in the high-temperature domain. The activation energy is positive above 600 K for both reactions as expected on the basis of earlier results on complex-forming bimolecular reactions. The TST calculations also yield a positive activation energy for both reactions above about 500 K, but the TST rate coefficients increase with the temperature

DOI: 10.1021/acs.energyfuels.8b00989
Energy Fuels 2018, 32, 10100−10105

significantly faster than the QCT rate coefficients. We have checked whether this is caused by some error arising because of the harmonic oscillator approximation used in the calculation of the partition function of the transition state. In particular, the contribution of the low-frequency modes to the partition function of the transition state located at the geometry of the submerged barrier were calculated by both the harmonic (shown in Figures 2 and 3) and the hindered rotor approximation,[36] but only minor differences were found that would not improve the TST prediction. The QCT results are more reliable because the QCT method properly describes the dynamics of the reaction, while TST is based on two assumptions that may not be fulfilled in these reactions. These assumptions are that, during the reaction, the system is always in equilibrium and that, if the system crosses the transition state (placed on the top of the potential barrier), it will never return. An indication of the inadequacy of the latter is that we detected numerous trajectories in which the system crossed the barrier but returned and re-formed the reactants.

The calculated rate coefficients for reaction $CH_3 + HBr \rightarrow CH_4 + Br$ (reaction R−2) are traced amazingly well by the curve described by eq 2 proposed by Burgess et al.[12] On the other hand, eq 1, which they use for reaction $OH + HBr \rightarrow H_2O + Br$ (reaction R6), significantly overestimates the rate coefficients.

CONCLUSION

QCT calculations were performed to determine the magnitude and temperature dependence of the rate coefficients for reactions $OH + HBr \rightarrow H_2O + Br$ (reaction R6) and $CH_3 + HBr \rightarrow CH_4 + Br$ (reaction R−2) using PES derived from accurate *ab initio* quantum chemical results. The dynamical calculations yielded rate coefficients that agree with the experimental results available around room temperature. In contrast to the negative activation energy observed earlier at lower temperatures, both k_6 and k_{-2} increase with an increasing temperature starting at about 600 K. The temperature dependence of the rate coefficients cannot be described by the Arrhenius expression, but the extended Arrhenius formula can be fit to them very well.

The QCT data support the assumption that the temperature dependence of the rate coefficient is not monotonous; the activation energy switches from negative at low temperatures to positive at about 600 K for both reactions. We found that the rate coefficients calculated by conventional TST are close to the experimental and QCT data at low temperatures for reaction R6, but they are larger by about a factor of 2 in this range for reaction R−2. The slope of the k versus T curves obtained by TST is too large by about a factor of 2 or more in the flame temperature range. This indicates that, for the calculation of the rate coefficients of these reactions, conventional TST is not reliable.

The comparison of the rate coefficients to those obtained by formulas proposed by Burgess et al. shows that eq 2 provides an almost perfect fit to the $CH_3 + HBr \rightarrow CH_4 + Br$ QCT rate coefficients, while eq 1 significantly overestimates the calculated rates for reaction $OH + HBr \rightarrow H_2O + Br$.

We propose eqs 5 and 6 to calculate the rate coefficients of reactions R6 and R−2, respectively, for use in flame inhibition models.

AUTHOR INFORMATION

Corresponding Author

*E-mail: lendvay.gyorgy@ttk.mta.hu.

ORCID

Gábor Czakó: 0000-0001-5136-4777

György Lendvay: 0000-0002-2150-0376

Notes

The authors declare no competing financial interest.

ACKNOWLEDGMENTS

This work has been supported by the State of Hungary, co-financed by the European Regional Development Fund, within Projects VEKOP-2.3.2-16-2017-00013 and K108966 at the Research Centre for Natural Sciences and within Project EFOP-3.6.1-16-2016-00015 at the University of Pannonia, and by the ÚNKP-17-2: New National Excellence Program of the Ministry of Human Capacities (to Szabolcs Góger), as well as COST Action 1404 SMARTCATs. Gábor Czakó thanks the National Research, Development and Innovation Office (NKFIH, K-125317) for financial support.

REFERENCES

(1) Alaee, M.; Arias, P.; Sjödin, A.; Bergman, Å. An Overview of Commercially Used Brominated Flame Retardants, Their Applications, Their Use Patterns in Different Countries/Regions and Possible Modes of Release. *Environ. Int.* **2003**, *29*, 683−689.

(2) Covaci, A.; Harrad, S.; Abdallah, M. A-E.; Ali, N.; Law, R. J.; Herzke, D.; de Wit, C. A. Novel Brominated Flame Retardants: A Review of Their Analysis, Environmental Fate and Behavior. *Environ. Int.* **2011**, *37*, 532−556.

(3) United Nations Environment Programme (UNEP). *Annex A to the Montreal Protocol*; UNEP: Nairobi, Kenya, 1994; http://ozone.unep.org/en/handbook-montreal-protocol-substances-deplete-ozone-layer/39 (accessed Feb 25, 2018).

(4) Gann, R. G. Guidance for Advanced Fire Suppression in Aircraft. *Fire Technol.* **2008**, *44*, 263−282.

(5) United Nations Environment Programme (UNEP). *Montreal Protocol on Substances that Deplete the Ozone Layer, 2010 Assessment Report of the Halons Technical Options Committee*; UNEP: Nairobi, Kenya, 2011; http://ozone.unep.org/en/Assessment_Panels/TEAP/Reports/HTOC/HTOC-Assessment-Report-2010.pdf (accessed Feb 25, 2018).

(6) United Nations Environment Programme (UNEP). *Montreal Protocol on Substances that Deplete the Ozone Layer, Report of the UNEP Halons Technical Options Committee*; UNEP: Nairobi, Kenya, Dec 2014; Vol. *1*, 2014 Assessment Report, http://ozone.unep.org/en/Assessment_Panels/TEAP/Reports/HTOC/HTOC%202014%20Assessment%20Report.pdf (accessed Feb 25, 2018).

(7) United Nations Environment Programme (UNEP). *The Kigali Amendment (2016): The Amendment to the Montreal Protocol Agreed by the Twenty-Eighth Meeting of the Parties (Kigali, 10−15 October 2016)*; UNEP: Nairobi, Kenya, 2016; http://ozone.unep.org/en/handbook-montreal-protocol-substances-deplete-ozone-layer/41453 (accessed Feb 25, 2018).

(8) Westbrook, C. K. Inhibition of Hydrocarbon Oxidation in Laminar Flames and Detonations by Halogenated Compounds. *Symp. (Int.) Combust., [Proc.]* **1982**, *19*, 127−141.

(9) Westbrook, C. K. Numerical Modeling of Flame Inhibition by CF_3Br. *Combust. Sci. Technol.* **1983**, *34*, 201−225.

(10) Noto, T.; Babushok, V. I.; Burgess, D. R. F.; Hamins, A.; Tsang, W.; Miiolek, A. Effect of Halogenated Flame Inhibitors on C_1-C_2 Organic Flames. *Symp. (Int.) Combust., [Proc.]* **1996**, *26*, 1377−1383.

(11) Babushok, V. I.; Linteris, G. T.; Burgess, D. R., Jr.; Baker, P. T. Hydrocarbon Flame Inhibition by $C_3H_2F_3Br$ (2-BTP). *Combust. Flame* **2015**, *162*, 1104−1112.

DOI: 10.1021/acs.energyfuels.8b00989
Energy Fuels 2018, 32, 10100−10105

(12) Burgess, D. R., Jr.; Babushok, V. I.; Linteris, G. T.; Manion, J. A. A Chemical Kinetic Mechanism for 2-Bromo-3,3,3-trifluoropropene (2-BTP) Flame Inhibition. *Int. J. Chem. Kinet.* **2015**, *47*, 533−619.
(13) de Oliveira-Filho, A. G. S.; Ornellas, F. R.; Bowman, J. M. Quasiclassical Trajectory Calculations of the Rate Constant of the OH + HBr → Br + H_2O Reaction Using a Full-Dimensional Ab Initio Potential Energy Surface Over the Temperature Range 5 to 500 K. *J. Phys. Chem. Lett.* **2014**, *5*, 706−712.
(14) Czakó, G. Accurate Ab Initio Potential Energy Surface, Thermochemistry, and Dynamics of the Br(^{2}P, $^2P_{3/2}$) + CH_4 → HBr + CH_3 Reaction. *J. Chem. Phys.* **2013**, *138*, 134301.
(15) de Oliveira-Filho, A. G. S.; Ornellas, F. R.; Bowman, J. M. Energy Disposal and Thermal Rate Constants for the OH + HBr and OH + DBr Reactions: Quasiclassical Trajectory Calculations on an Accurate Potential Energy Surface. *J. Phys. Chem. A* **2014**, *118*, 12080−12088.
(16) Mozurkewich, M.; Benson, S. W. Negative Activation Energies and Curved Arrhenius Plots. 1. Theory of Reactions Over Potential Wells. *J. Phys. Chem.* **1984**, *88*, 6429−6435.
(17) Troe, J. The Polanyi Lecture: The Colorful World of Complex-forming Bimolecular Reactions. *J. Chem. Soc., Faraday Trans.* **1994**, *90*, 2303−2317.
(18) Chen, J.; Rauk, A.; Tschuikow-Roux, E. On the Question of Negative Activation Energies: Absolute Rate Constants by RRKM and G1 Theory for CH_3 + HX → CH_4 + X (X = Cl, Br) Reactions. *J. Phys. Chem.* **1991**, *95*, 9832−9836.
(19) Krasnoperov, L. M.; Peng, J.; Marshall, P. Modified Transition State Theory and Negative Apparent Activation Energies of Simple Metathesis Reactions: Application to the Reaction CH_3 + HBr → CH_4 + Br. *J. Phys. Chem. A* **2006**, *110*, 3110−3120.
(20) Raff, L. M.; Thompson, D. L. In *Theory of Chemical Reaction Dynamics*; Baer, M., Ed.; CRC Press: Boca Raton, FL, 1985; Vol. 3, pp 1−122.
(21) Szabó, P.; Lendvay, G. A Quasiclassical Trajectory Study of the Reaction of H Atoms with $O_2(^1\Delta_g)$. *J. Phys. Chem. A* **2015**, *119*, 7180−7189.
(22) Szabó, P.; Lendvay, G. The Dynamics of Complex-Forming Bimolecular Reactions: a Comparative Theoretical Study of the Reactions of H atoms with $O_2(^3\Sigma_g^-)$ and $O_2(^1\Delta_g)$. *J. Phys. Chem. A* **2015**, *119*, 12485−12497.
(23) Lahankar, S. A.; Zhang, J.; Minton, T. K.; Guo, H.; Lendvay, G. Dynamics of the O-Atom Exchange Reaction $^{16}O(^3P)$ + $^{18}O^{18}O(^3\Sigma_g^-)$ → $^{16}O^{18}O(^3\Sigma_g^-)$ + $^{18}O(^3P)$ at Hyperthermal Energies. *J. Phys. Chem. A* **2016**, *120*, 5348−5359.
(24) Seinfeld, J. I.; Francisco, J. S.; Hase, W. L. *Chemical Kinetics and Dynamics*; Prentice Hall: Englewood Cliffs, NJ, 1989.
(25) Braams, B. J.; Bowman, J. M. Permutationally Invariant Potential Energy Surfaces in High Dimensionality. *Int. Rev. Phys. Chem.* **2009**, *28*, 577−606.
(26) Mullen, C.; Smith, M. A. Temperature Dependence and Kinetic Isotope Effects for the OH+HBr Reaction and H/D Isotopic Variants at Low Temperatures (53−135 K) Measured Using a Pulsed Supersonic Laval Nozzle Flow Reactor. *J. Phys. Chem. A* **2005**, *109*, 3893−3902 and references therein.
(27) Andersen, H. C.; Kistiakowsky, G. B. The Activation Energy of the Reaction CH_3+HBr = CH_4+Br and the Carbon−Hydrogen Bond Strength in Methane. *J. Chem. Phys.* **1943**, *11*, 6−10.
(28) Williams, R. R., Jr.; Ogg, R. A., Jr. Kinetics of the Photolysis of Methyl Iodide and the Hydrogen Halides II. Photolysis of Methyl Iodide in the Presence of Iodine and the Hydrogen Halides. *J. Chem. Phys.* **1947**, *15*, 696−702.
(29) Fettis, G. C.; Trotman-Dickenson, A. F. The Reactions of Methyl and Ethyl Radicals with Hydrogen Bromide and the Strength of C−H bonds. *J. Chem. Soc.* **1961**, *0*, 3037−3041.
(30) Russell, J. J.; Seetula, J. A.; Gutman, D. Kinetics and Thermochemistry of Methyl, Ethyl, and Isopropyl. Study of the Equilibrium R + HBr ⇌ R-H + Br. *J. Am. Chem. Soc.* **1988**, *110*, 3092−3099. Note that the rate coefficients reported in this paper were shown to be too low by about a factor of 2 in ref 32.
(31) Nicovich, J. M.; Van Dijk, C. A.; Kreutter, K. D.; Wine, P. H. Kinetics of the Reactions of Alkyl Radicals with Hydrogen Bromide and Deuterium Bromide. *J. Phys. Chem.* **1991**, *95*, 9890−9896.
(32) Seakins, P. W.; Pilling, M. J.; Niiranen, J. T.; Gutman, D.; Krasnoperov, L. N. Kinetics and Thermochemistry of R + Hydrogen Bromide ⇌ RH + Bromine Atom Reactions: Determinations of the Heat of Formation of Ethyl, Isopropyl, sec-Butyl and tert-Butyl Radicals. *J. Phys. Chem.* **1992**, *96*, 9847−9855.
(33) Seetula, J. A. Kinetics of the R + HBr → RH + Br (R = CH_2I or CH_3) Reaction. An Ab Initio Study of the Enthalpy of Formation of the CH_2I, CHI_2 and CI_3 Radicals. *Phys. Chem. Chem. Phys.* **2002**, *4*, 455−460.
(34) Sheng, L.; Li, Z.-S.; Liu, J.-Y.; Sun, C.-C. Computational Study of the Rate Constants and Kinetic Isotope Effects for the CH_3 + HBr → CH_4 + Br Reaction. *J. Chem. Phys.* **2003**, *119*, 10585−10590.
(35) Smith, I. W. M. *Kinetics and Dynamics of Elementary Gas Reactions*; Butterworth & Co.: Boston, MA, 1980; Butterworths Monographs in Chemistry and Chemical Engineering.
(36) Ayala, P. Y.; Schlegel, B. H. Identification and Treatment of Internal Rotation in Normal Mode Vibrational Analysis. *J. Chem. Phys.* **1998**, *108*, 2314.

DOI: 10.1021/acs.energyfuels.8b00989
Energy Fuels 2018, 32, 10100−10105